Dehydration behavior and kinetics of kurnakovite under microwave irradiation

Fatma Tuğçe ŞENBERBER[1,2], **Meral YILDIRIM**[1], **İklim Nergiz ÖZDOĞAN**[1],
Azmi Seyhun KIPÇAK[1], **Emek DERUN**[1,*]
[1]Department of Chemical Engineering, Yıldız Technical University, İstanbul, Turkey
[2]Program of Occupational Health and Safety, Ataşehir Adıgüzel Vocational School of Higher Education,
İstanbul, Turkey

Abstract: In this research, the dehydration behavior of kurnakovite was studied under microwave irradiation. The kinetic parameters of the dehydration reaction were determined using different kinetic models. Kurnakovite was characterized by the techniques of X-ray diffraction (XRD), Fourier transform infrared spectroscopy (FT-IR), and scanning electron microscopy (SEM) before and after the dehydration process. According to the results, kurnakovite was identified as a compound with the powder diffraction file (pdf) number 00-024-0700 before the dehydration process and after the dehydration process amorphous formations were observed. Moreover, FT-IR results showed that dehydration was completed successfully because of the disappearance in the band values of structural water. The dehydration process was ended at 25, 20, and 15 min for the power levels of 360, 600, and 800 W, respectively. Among the models, the two-term exponential model best fits the drying experimental data. For the activation energy calculation, the Page model best fits the experimental data and was found as 9.92 W $\times$ g^{-1}.

Key words: Dehydration, kinetic, kurnakovite, microwave

1. Introduction

There are more than 200 different combinations of boron atoms with other elements and the natural forms of these combinations are known as boron minerals.[1] Boron minerals can be used in the areas of glass, abrasives and refractories, agriculture, cleaning compounds and bleaches, flame retardants, fuels, medicines, metallurgy, and nuclear applications.[2] Therefore, determination of the characteristic properties of boron minerals is important. Boron minerals are classified according to the metal atom in the structure, such as sodium borates, calcium borates, and magnesium borates. Kurnakovite ($Mg_2B_6O_{11} \cdot 15H_2O$ or $2Mg(B_3O_3(OH)_5) \cdot 5H_2O$) is a kind of magnesium borate hydrate mineral that has a white appearance and a triclinic crystal system. Kurnakovite has strong features in neutron shielding compared to other types of borates.[3,4] It also has a polymorph of inderite, which has the same chemical formula with a different lattice structure. According to the thermal analyses of inderite, the dehydration process was completed at lower than 400 °C and the total mass loss was 47.20%.[5,6]

The heating mechanism of materials can be explained by the dipolar polarization mechanism, the conduction mechanism, and the interphase polarization mechanism.[7] The microwave heating process emerges via the dipolar polarization mechanism.[8] Microwaves are the wavelengths in the range of 1 mm to 1 m and frequencies of 0.3 to 300 GHz. Microwave irradiation can be used in the synthesis of organic and inorganic compounds,

*Correspondence: moroydor@yildiz.edu.tr

polymers, biochemical, radioisotopes, etc. The literature indicates that there are several applications of microwave irradiation in material science, nanotechnology, ceramics, medicinal chemistry, green chemistry, and dehydration.[9−23]

During conventional drying, heat is transferred from outside to inside, which is in the opposite direction of steam diffusion, causing low drying efficiency. As a result, conventional drying takes a long time and consumes high amounts of energy.[10] In microwave drying, on the other hand, heat is transferred from inside to outside. Microwave dehydration behavior on different types of minerals such as zeolites, ilmenite, goethite, ulexite, borax, and boric acid was studied in the literature.[20−25] Li et al. studied the effects of power level and sample mass on the microwave drying characteristics of ilmenite.[20] Roussy et al. determined the dehydration kinetic model of 13X zeolite as first order.[21] Saito et al. researched the dehydration behavior of goethite mineral blended with graphite at different mole ratios.[22] Eymir and Okur showed that ulexite mineral could be dried using microwave energy.[23] Kocakusak et al. studied the microwave dehydration of boric acid in the range of 100–700 W.[24] Ozdogan et al. researched the microwave dehydration behavior of the mineral inderite, which has the same chemical formula in a different lattice structure. Inderite has a monoclinic crystal system, whereas kurnakovite has a triclinic crystal system. In the crystal system of inderite, the obtained data are not suitable for the calculation of kinetic parameters because the entire structural water cannot be removed.[26]

The novelty of this research is the determination of the dehydration behavior and kinetic parameters of kurnakovite under microwave irradiation. Besides kinetic studies, the obtained compounds were characterized by different instrumental techniques.

2. Results and discussion

2.1. Characterization results of pure and dehydrated kurnakovite

The raw material used in experiment is identified as kurnakovite with the chemical formula $Mg_2B_6O_{11}\cdot15H_2O$ and the powder diffraction file (pdf) number 00-024-0700. The crystallographic data of kurnakovite are given in Table 1.

Table 1. Crystallographic data of kurnakovite.

Mineral name	Kurnakovite
Pdf no.	00-024-0700
Chemical formula	$Mg_2B_6O_{11}\cdot15H_2O$
Molecular weight (g/mol)	559.6986
Crystal system	Anorthic
a (Å)	8.1500
b (Å)	10.5700
c (Å)	6.2500
α (°)	96.52
β (°)	106.02
γ (°)	106.47
Density (calculated) (g cm^{-3})	1.91

The X-ray diffraction (XRD) pattern of pure kurnakovite and dehydrated minerals at different power levels can be seen in Figure 1. The characteristic peaks (h k l [d$_{spacing}$]) of kurnakovite were observed at the 2θ positions of 12.28° (–1 1 1 [7.20 Å]), 17.98° (–1 2 0 [4.93 Å]), 22.49° (–2 1 0 [3.95 Å]), and 31.25° (2 –2

1 [2.86 Å]). After the microwave treatment, the dehydrated sample cannot be determined by XRD due to the lack of characteristic peak observation, which indicates amorphous structure formation.
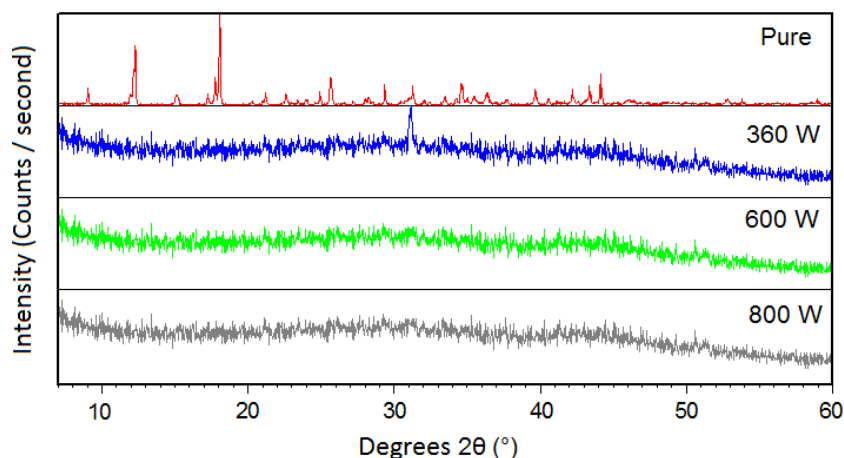

Figure 1. XRD pattern of pure and dehydrated kurnakovite samples.

The Fourier transform infrared (FT-IR) spectra of pure and dehydrated kurnakovite are shown in Figure 2. For IR peaks of hydrated boron minerals, the peaks at about 3200 and 1680 cm^{-1} are the characteristic band values of structural water content. After microwave treatment, these kinds of band values get lower, which indicates the removal of water from the structure. The peak at 1340 cm^{-1} is ascribed to asymmetric stretching of three coordinate boron to oxygen bands [ν_{as} (B$_{(3)}$–O)]. The bending mode of boron–oxygen–hydrogen [δ (B–O–H)] is fitted in the band values around 1200 cm^{-1}; however, this kind of characteristic vibration disappeared in the spectra of dehydrated mineral, which can be explained by the effects of microwaves. Asymmetric stretching of four coordinate boron to oxygen bands [ν_{as} (B$_{(4)}$–O)] is seen between 1009 cm^{-1} and 991 cm^{-1}. The symmetric stretching of three coordinate boron to oxygen bands [ν_s (B$_{(3)}$–O)] is observed in the range of 880–812 cm^{-1}. The frequency at 704 cm^{-1} belongs to symmetric stretching of four coordinate boron to oxygen bands [ν_s (B$_{(4)}$–O)].[27]
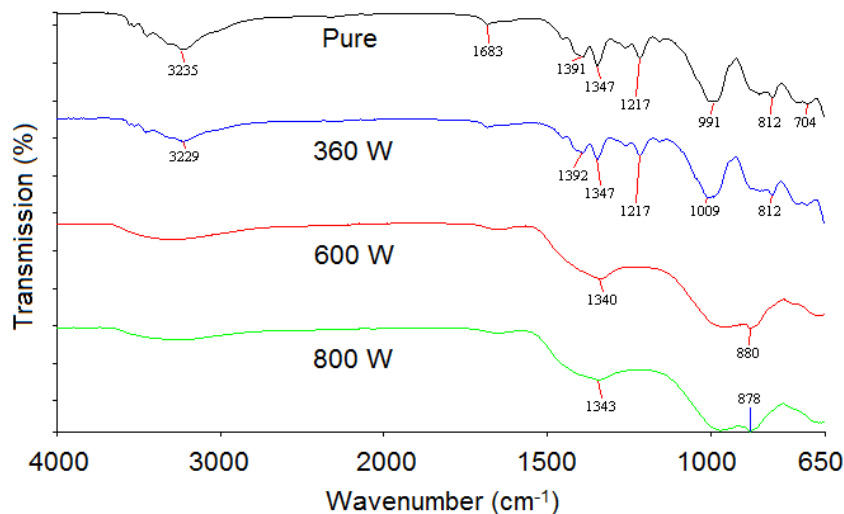

Figure 2. FT-IR spectra of pure and dehydrated kurnakovite.

Scanning electron microscope (SEM) surface morphologies of pure and dehydrated kurnakovite are presented in Figure 3. According to the SEM images, pure kurnakovite is in microscale and particles have multiangular and overlapped shapes. The particle morphology is similar to that of the pure mineral after microwave dehydration; however, particles size is in submicro scale with the removal of structural water. Particle size of dehydrated kurnakovite is in the range of 500 nm–1.5 μm, whereas that of pure mineral is between 1 and 3 μm.
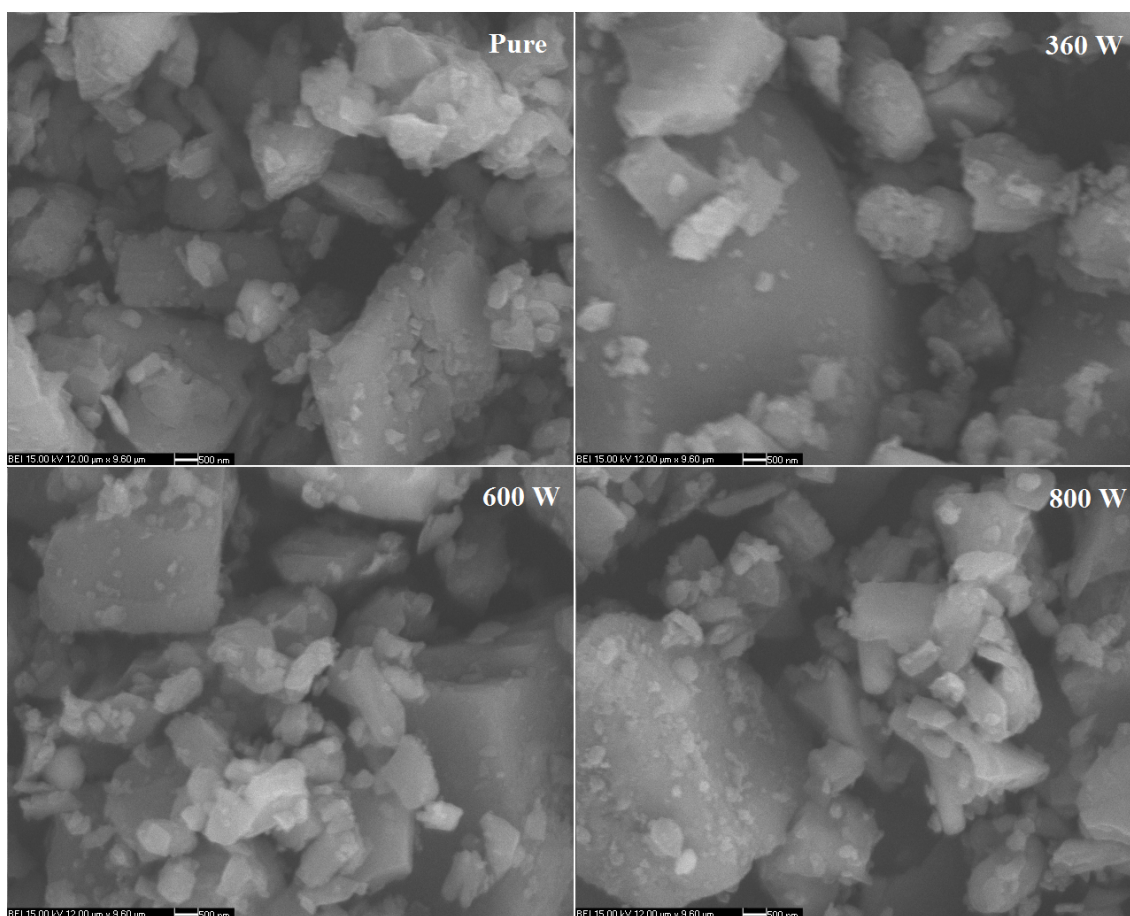

Figure 3. SEM morphologies of pure and dehydrated kurnakovite.

2.2. Mathematical modelling results of the dehydration studies

2.2.1. Structural water content

The effects of different microwave power levels on the structural water dehydration of kurnakovite are shown in Figure 4.

The initial average SW of kurnakovite was 0.9320 kg structural water/kg dehydrated mineral, and the initial average SW decreased to 0.0162, 0.0141, and 0.0133 kg structural water/kg dehydrated mineral for the microwave power levels of 360, 600, and 800 W, respectively. The plot type of the dehydration curves is similar to those in previous studies.[20,28]

From Figure 4, it is seen that an increase in microwave power leads to a decrease in dehydration time. The dehydration times for achieving the dehydrated content in kurnakovite were 25, 20, and 15 min for the microwave power levels of 360, 600, and 800 W, respectively.
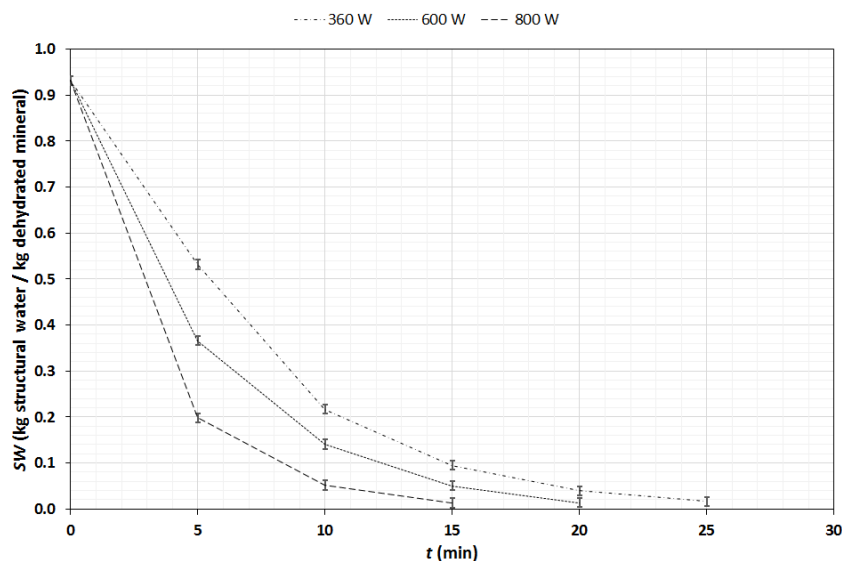
Figure 4. Structural water dehydration of kurnakovite by different power levels.

It is seen that higher heat absorption was obtained with higher microwave power. This means that the higher heat absorption causes higher product temperature, higher mass transfer driving force, faster drying rates, and shorter drying times.[28]

2.2.2. Dehydration rate

In Figure 5, the plot of dehydration rate and structural water for kurnakovite is presented. Generally, the dehydration processes of hydrate structures include the rising rate, constant, and falling periods.[20] However, in the dehydration of kurnakovite no constant rate period was observed. At 360, 600, and 800 W, the rising rate period was observed at the SW values between 0.9320 and 0.5315 kg structural water/kg dehydrated mineral, 0.9320 and 0.3663 kg structural water/kg dehydrated mineral, and 0.9320 and 0.1986 kg structural water/kg dehydrated mineral, respectively. Likewise, the falling rate period was observed at the SW values between 0.5315 and 0.0.0162 kg structural water/kg dehydrated mineral, 0.3663 and 0.0141 kg structural water/kg dehydrated mineral, and 0.1986 and 0.0133 kg structural water/kg dehydrated mineral for 360, 600, and 800 W, respectively.

2.2.3. Evaluation of the models

The Henderson and Pabis, Lewis, logarithmic, Midilli, modified Page, Page, and two-term exponential models were fitted to the experimental structural water ratio (SWR) with respect to dehydration times. Based on the highest R^2 and lowest χ^2 and RMSE values the best models were selected. In Table 2, the statistical results and calculated model constants are given. The highest and lowest R^2 values are obtained as 0.999999 and 0.968858. The values of χ^2 and RMSE are close to 0, meaning that the calculated data perfectly fit the experimental data. Among the models, the two-term exponential model best fits the experimental SWR. The plot of experimental SWR and calculated SWR for the methods of the two-term exponential model is presented in Figure 6.

In Figure 6, the obtained data are found on a nearly 45° straight line, meaning that there is good agreement between the experimental and the calculated SWR values.
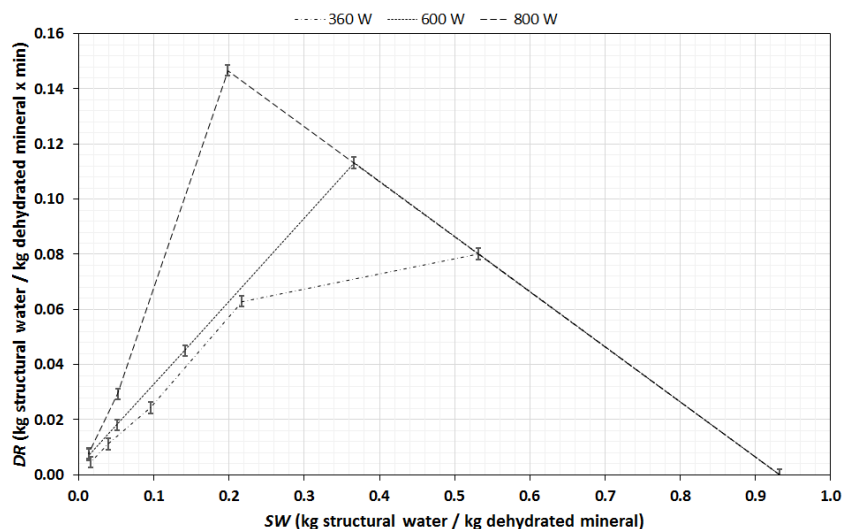
Figure 5. The plot of dehydration rate and structural water for kurnakovite.
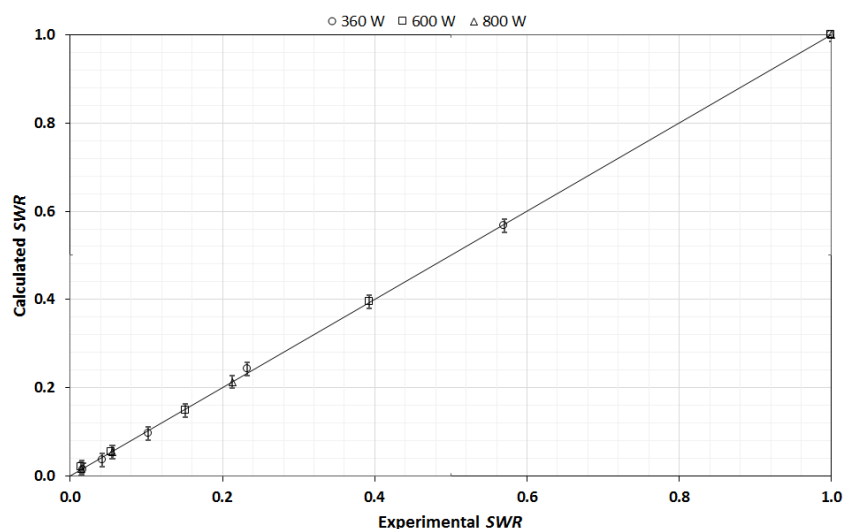

Figure 6. Experimental SWR and calculated SWR for the two-term exponential model.

2.2.4. Activation energy result

Activation energy can be calculated from the slope of the $\ln(k)$ versus m/P plot, which is given in Figure 7. E_a and k_0 values are calculated as 9.92 W $\times$ g^{-1} and 1.0975 min^{-1}, respectively, using the Page model, whose R^2 value (0.9634) is higher than that of any other models.

In conclusion, the dehydration behavior of kurnakovite was investigated using microwaves and kinetic parameters were calculated. Several microwave power levels were used for the dehydration experiments and seven different models were applied to the dehydration data in order to model the obtained data. Characterization experiments of pure and dehydrated kurnakovite were conducted using the techniques of XRD, FT-IR, and SEM. From the characterization analyses, kurnakovite was found as pure crystal phase with a pdf number of 00-024-0700 and after the dehydration experiments, the phase of kurnakovite was changed to amorphous and the

Table 2. Estimated coefficients and statistical data obtained from different models.

Model	Power (W)	360	600	800
Henderson and Pabis	a	1.018666	1.001042	0.999520
	k	0.137993	0.188942	0.305208
	R^2	0.996095	0.999927	0.999918
	χ^2	0.001458	0.000032	0.000053
	RMSE	0.031181	0.004364	0.0051264
Midilli	a	1.000659	0.999998	1.000000
	k	0.067465	0.185026	2.709210
	n	1.330370	1.002026	33.69387
	b	0.000605	−0.000456	0.005250
	R^2	0.999848	0.999999	0.968858
	χ^2	0.000076	2.80×10^{-8}	0.039068
	RMSE	0.006166	0.000106	0.098828
Lewis	k	0.135927	0.188789	0.305297
	R^2	0.995842	0.999927	0.999917
	χ^2	0.001242	0.000024	0.000035
	RMSE	0.032176	0.004390	0.005132
Logaritmic	a	1.064422	1.010186	0.991405
	k	0.121038	0.183504	0.314227
	c	−0.052876	−0.010253	0.008461
	R^2	0.997607	0.999999	0.999976
	χ^2	0.001192	2.34×10^{-7}	0.000031
	RMSE	0.024416	0.000306	0.002785
Modified Page	k	0.138312	0.186672	0.323216
	n	1.204083	1.035392	0.907232
	R^2	0.996253	0.999974	0.999999
	χ^2	0.001216	0.000012	0.000001
	RMSE	0.028469	0.002639	0.000551
Page	k	0.072924	0.175906	0.358918
	n	1.282030	1.035392	0.907232
	R^2	0.999710	0.999974	0.999999
	χ^2	0.000108	0.000012	0.000001
	RMSE	0.008493	0.002639	0.000551
Two-term exponential	a	1.890104	1.373804	0.550574
	k	0.196920	0.209097	0.414077
	R^2	0.999868	0.999977	0.999997
	χ^2	0.000049	0.000010	1.66×10^{-6}
	RMSE	0.005728	0.002472	0.000911

particle sizes were decreased. Furthermore, some bands in the FT-IR spectra disappeared after the dehydration experiments. From the dehydration data, it was seen that kurnakovite is dehydrated at a time of 25, 20, and 15 min at microwave power levels of 360, 600, and 800 W and no constant rate period was observed during the dehydration experiments. Among the seven different models, the Page model best fit the dehydration data obtained and using this model the activation energy of kurnakovite was calculated as 9.92 W $\times$ g^{-1}.
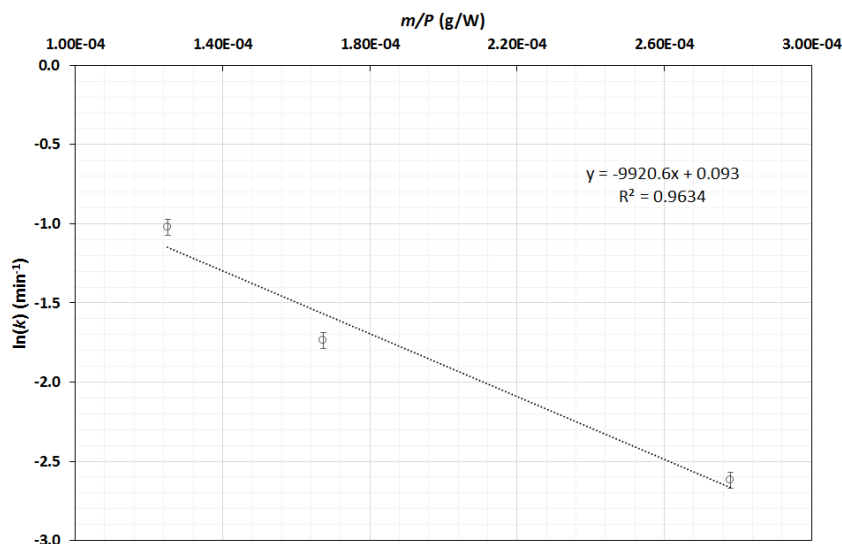
Figure 7. The plot of kurnakovite mass over microwave power level versus structural water loss rate constant obtained by the Page model.

3. Experimental

3.1. Raw material preparation and characterization

Kurnakovite was obtained from Bandırma Boron Works (Eti Maden, Balıkesir, Turkey) with the purity of 99%. Before the experiments, the mineral was ground with a Retsch RM 100 (Retsch GmbH & Co KG, Haan, Germany) and sieved through a Fritsch analysette 3 Spartan pulverisette 0 vibratory sieve-shaker (Fritsch, Idar-Oberstein, Germany) to obtain a particle size below 75 μm.

The characterization studies of the pure mineral and the products obtained after the dehydration studies were implemented by XRD, FT-IR, and SEM techniques. XRD analysis was applied by PANalytical Xpert Pro (PANalytical B.V., Almelo, the Netherlands) XRD at 45 kV and 40 mA ($\lambda = 0.15318$ nm) using Cu-Kα radiation in the 2θ range of 7–60° to identify the mineral. The spectroscopic analysis was carried out in the range of 4000 cm^{-1}–650 cm^{-1}. A PerkinElmer Spectrum One FT-IR (PerkinElmer, MA, USA) with universal attenuation total reflectance (ATR) sampling accessory with a diamond/ZnSe crystal was used to record the infrared spectrum of kurnakovite. The morphological properties were investigated using a CamScan Apollo 300 Field-Emission SEM (CamScan, Oxford, United Kingdom) at 15 kV with a backscattering electron detector (BEI) and the magnification was set to 10,000.

3.2. Microwave dehydration procedure

Microwave dehydration studies were carried with a laboratory-type custom microwave oven that has an output power of 800 W and a working frequency of 2450 MHz. In experiments, power levels were determined as 360, 600, and 800 W. A determined amount of kurnakovite was exposed to microwave radiation and the mineral was weighed at 5-min intervals until a constant weight was obtained.

The structural water percentage of kurnakovite was determined as 48.24%, which is equal to 0.9320 kg structural water/kg dehydrated mineral, according to thermal analyses results in the literature.[26]

3.3. Mathematical modelling of the dehydration studies

The structural water content (SW) (kg structural water/kg dehydrated mineral), dehydration rate (DR) (kg structural water/kg dehydrated mineral × min), and structural water ratio (SWR) (dimensionless) of kurnakovite were calculated using Eqs. (1)–(3):

$$SW = \frac{w_{sw}}{w_d} \tag{1}$$

$$DR = \frac{SW_{t+dt} - SW_t}{dt} \tag{2}$$

$$SWR = \frac{SW_t - SW_e}{SW_i - SW_e}, \tag{3}$$

where w_{sw} is the structural water amount (g); w_d is the dehydrated mineral amount (g); SW_{t+dt} is the structural water amount at $t + dt$ (kg structural water/kg dehydrated mineral); t is the dehydration time (min); and SW_t, SW_e, and SW_i are the structural water content at selected time, at equilibrium, and at the initial value. Since the SW_e is approximately zero, SW_e is neglected in the calculation of SWR.

The dehydration curves obtained from different microwave power levels were fitted to seven different models, which are given in Table 3.

Table 3. Models used for fitting the experimental data.

Model	Equation	Reference
Henderson and Pabis	$SWR = a \times \exp\left(-k \times t\right)$	27
Lewis	$SWR = \exp\left(-kt\right)$	28
Logarithmic	$SWR = a \times \exp\left(-k \times t\right) + c$	29
Midilli	$SWR = a \times \exp\left(-k \times t^n\right) + b \times t$	30
Modified Page	$SWR = \exp\left((-kt)^n\right)$	31
Page	$SWR = \exp\left(-kt^n\right)$	29, 30
Two-term exponential	$SWR = a \times \exp\left(-kt\right) + (1 - a) \times \exp\left(-k \times a \times t\right)$	32

k is the structural water loss rate constant or coefficient ($\min^{-1}$) and a, b, c, and n are the constants (dimensionless)

A nonlinear regression analysis based on the Lavenberg–Marquardt algorithm was used for the estimation of model parameters using Statistica 8.0 (StatSoft Inc., Tulsa, OK, USA). The calculated data using the seven different models were evaluated using the coefficient of determination (R^2), reduced chi-square (χ^2), and root mean square error (RMSE). High R^2 values and low χ^2 and RMSE values were accepted as better results.[33] χ^2 and RMSE equations are given in Eqs. (4) and (5), respectively:

$$\chi^2 = \frac{\sum\limits_{i=1}^{N} \left(SWR_{exp,i} - SWR_{calc,i}\right)^2}{N - z} \tag{4}$$

$$RMSE = \left(\frac{1}{N} \sum\limits_{i=1}^{N} \left(SWR_{pre,i} - SWR_{calc,i}\right)^2\right)^{1/2}, \tag{5}$$

where SWR_{exp} and SWR_{calc} represent experimental and calculated values of structural water content ratios, respectively. N is the total number of experiments and z is the number of constants in the model.

3.4. Activation energy calculation

Activation energy of the kurnakovite can be calculated using the kinetic parameter k obtained from different models by the Arrhenius's equation given in Eq. (6):[32]

$$k = k_0 \times \exp\left(\frac{-E_a \times m}{P}\right), \tag{6}$$

where k can be defined as the structural water loss rate constant or coefficient (min^{-1}), k_0 is the pre-exponential constant (min^{-1}), E_a is the activation energy $(\text{W} \times \text{g}^{-1})$, P is the microwave power level (W), and m is the mass of kurnakovite (g).

References

1. Beatty, R. *Boron*; Marshall Cavendish Corporation: Tarrytown, NY, USA, 2006.

2. Garrett, D. E. *Borates: Handbook of Deposits, Processing, Properties, and Use*; Academic Press: London, UK, 1998.

3. Derun, E. M.; Kipcak, A. S. *J. Radioanal. Nucl. Chem.* **2012**, *292*, 871-878.

4. Zhou, B.; Michaelis, V. K.; Pan, Y.; Yao, Y.; Tait, K. T.; Hyde, B. C.; Wren, J. E. C.; Sherriff, B. L.; Kroeker, *S. Am. Mineral.* **2012**, *97*, 1858-1865.

5. Abdullaev, G. K.; Abbasov, B. E.; Rza-Zade, P. F. *Issled. Obl. Neorg. Fiz. Khim.* **1971**, 147-52.

6. Frost, R. L.; Lopez, A.; Xi, Y., Lima, R. M. F.; Scholz, R.; Granja, A. *Spectrochim. Acta Mol. Biomol. Spectrosc.* **2013**, *116*, 160-164.

7. Gabriel, C.; Gabriel, S.; Grant, E.; Halstead, B.; Mingos, D. *Chem. Soc. Rev.* **1998**, *27*, 213-223.

8. Adnadjevic, B.; Jovanovic, J. In *Advances in Induction and Microwave Heating of Mineral and Organic Materials*; Grundas, S., Ed. Intech: Croatia, 2011, pp. 392-420.

9. Loupy, A. *Microwave in Organic Synthesis*; Wiley–VCH: Weinheim, Germany, 2002.

10. Kipcak, A. S.; Derun, E. M.; Piskin, S. *J. Chem.* **2013**, Article ID *329238*, 1-6.

11. Bogdal, D.; Prociak, A. *Microwave-Enhanced of Polymer Chemistry and Technology*; Blackwell Pub: Oxford, UK, 2007.

12. Perelaer, J.; de Gans, B.; Schubert, U. *Adv. Mater.* **2006**, *18*, 2101-2104.

13. Tsuji, M.; Hashimoto, Y.; Nishizawa, Y.; Kubokawa, M.; Tsuji, T. *Chem. Eur. J.* **2005**, *1*, 440-452.

14. Li, J.; Jin, Y. L.; Zhang, X. G.; Yang, H. *Solid State Ionics* **2007**, *178*, 1590-1594.

15. Elander, N.; Jones, J.; Lu, S.; Stone-Elander, S. *Chem. Soc. Rev.* **2000**, *29*, 239-249.

16. Shipe, W.; Wolkenberg, S.; Linfsley, C. *Nature Rev. Drug Discov. Today Technol.* **2005**, *2*, 155-161.

17. Collins, J.; Leadbeater, N. *Org. Biomol. Chem.* **2007**, *5*, 1141-1150.

18. Nüchten, M.; Ondruschka, B.; Bonrath, W.; Gum, A. *Green Chem.* **2004**, *6*, 128-141.

19. Vanderah, T. *Science*, **2002**, *298*, 1182-1184.

20. Li, Y.; Lei, Y.; Zhang, L.; Peng, J.; Li, C. *Trans. Nonferrous Met. Soc. China*, **2011**, *21*, 202-207.

21. Roussy, G.; Zoulalian A.; Charreyre, M.; Thiebaut J. *J. Phys. Chem.* **1984**, *88*, 5702-5708.

22. Saito, Y.; Kawahira, K.; Yoshikawa, N.; Todoroki, H.; Taniguch, S. *ISIJ Int.* **2011**, *51*, 878-883.

23. Eymir, Ç.; Okur, H. *Thermochim. Acta* **2005**, *428*, 125-129.

24. Kocakusak, S.; Koroglu, H. J.; Tolun, R. *Chem. Eng. Process.* **1998**, *37*, 197-201.

25. Kocakusak, S.; Koroglu H. J.; Gozmen, T.; Savascı, O. T.; Tolun R. *Ind. Eng. Chem. Res.* **1996**, *35*, 159-163.

26. Ozdogan, I. N.; Aksoy, Y. T.; Senberber, F. T., Kipcak, A. S.; Piskin, M. B.; Derun, E. M. *CBU J. Sci.* **2016**, *11*, 373-377.

27. Jia, Y.; Gao, S.; Xia, S.; Li, L. *Spectrochim. Acta Part A* **2000**, *56*, 1291-1297.

28. Hammouda, I.; Mihoubi, D. *Energ. Convers. Manage.* **2014**, *87*, 832-839.

29. Godlevsky, M. N. *Comptes Rendus (Doklady) de l'Académie des Sciences de l'URSS* **1940**, *28,* 638-640.

30. Henderson, S. M.; Pabis, S. *J. Agr. Eng. Res.* **1961**, *6*, 169-174.

31. Roberts, J. S.; Kidd, D. R.; Padilla-Zakour, O. *J. Food Eng.* **2009**, *89*, 460-465.

32. Dadalı, G.; Apar, D. K.; Özbek, B. *Drying Technol.* **2007**, *25*, 917-924.

33. Doymaz, İ.; Kipcak, A. S.; Piskin, S. *Czech J. Food Sci.* **2015**, *33*, 367-376.

34. Midilli, A.; Kucuk, H.; Yapar, Z. *Drying Technol.* **2002**, *20*, 1503-1513.

35. Yaldız, O.; Ertekin, C.; Uzun, H. İ. *Energy* **2001**, *26*, 457-465.